

## Enhancing the resolution of scanning near-field optical microscopy by a metal tip grown on an aperture probe

Heinrich G. Frey,<sup>a)</sup> Fritz Keilmann, Armin Kriele,<sup>b)</sup> and Reinhard Guckenberger  
*Max-Planck-Institut für Biochemie, Abt. Molekulare Strukturbiologie, 82152 Martinsried, Germany*

(Received 5 August 2002; accepted 24 October 2002)

We show improvement of the optical and topographical resolution of scanning near-field optical microscopy by introducing a “tip-on-aperture” probe, a metallic tip formed on the aperture of a conventional fiber probe. The tip concentrates the light passing through the aperture. Thus the advantages of aperture and apertureless scanning near-field optical microscopy are combined. Tips are grown by electron beam deposition and then covered with metal. Fluorescent beads are imaged with a resolution down to 25 nm (full width at half maximum) in the optical signal. The near-field appears strongly localized within 5 nm in  $z$  direction, thus promising even higher resolution with sharper tips. © 2002 American Institute of Physics. [DOI: 10.1063/1.1530736]

“Conventional” scanning near-field optical microscopy achieves a resolution beyond the diffraction limit of conventional optical microscopy by using a subwavelength aperture probe scanning a few nanometers above the sample. However, the light throughput diminishes very strongly with decreasing aperture diameter<sup>1</sup> and cone angle of the probe, so a resolution  $<50$  nm is rarely seen in practice.<sup>2</sup> An additional problem is the usual metal film with thickness in the range of 100 nm which makes aperture probes broad, leads to relatively poor topographical resolution, and restricts optical imaging to flat samples.

Apertureless scanning near-field optical microscopes (SNOMs) obtain a much better resolution (1–10 nm)<sup>3–5</sup> by concentrating light fields close to the tip apex. The resolution corresponds to the apex radius  $a$ . However, the far-field illumination by a focused laser beam exposes a large area around the tip apex. This generates a large background scattering signal, which can, however, be suppressed by modulation techniques.<sup>6–9</sup> Moreover, in fluorescence imaging<sup>10–13</sup> a large area bleaching may result. Both disadvantages are overcome in the “tip-on-aperture” (TOA) approach demonstrated in this letter, where the tip is illuminated by a contiguous aperture.<sup>14–16</sup> The tip can be positioned and tailored to optimally concentrate at its apex the light fields provided by the aperture, fully exploiting plasmon<sup>14–17</sup> and antenna<sup>18</sup> resonances. A properly engineered TOA probe will combine the advantages of aperture and apertureless probes, thus achieving low background and high optical as well as topographical resolution. In this letter we describe the results with a TOA probe by demonstrating high resolution and strong near-field signals with a fluorescent sample.

To produce the TOA probe we start by thinning an optical monomode fiber (3M, FS-SN-3224) in an etching solution (40% HF:H<sub>2</sub>O:40% NH<sub>4</sub>F=1:1:1) for 100 min. Then, the fiber is etched in a fourfold diluted solution to a diameter of 15  $\mu\text{m}$ . As the fiber core etches more slowly than the cladding, a sharp tip of 2  $\mu\text{m}$  length results, as described before with a Ge-doped fiber.<sup>19</sup> The tip is covered on all

sides with a few nm of Cr for adhesion, and then with about 200 nm Au, chosen for its good contrast in a scanning electron microscope (SEM). An aperture is opened by pressing the tip on a glass surface and monitoring the far-field light throughput.

To form the tip of the TOA probe, we focus the electron beam of a SEM (JEOL 5600) on the center of the aperture for about 7 s, at 8 kV acceleration voltage, thereby growing an electron-beam-deposited tip (EBD tip)<sup>20</sup> [Fig. 1(a)]. Such tips are also called contamination tips because they build up from inevitable trace impurities. Layers of 3.5 nm Cr and 33 nm Al are then deposited by evaporation at 45° incidence [Fig. 1(b)]. In this way the EBD tip is metallized on one side, and the original aperture is reduced to a small and elongated aperture left by the tip’s shadow, resulting in an asymmetric tip–aperture arrangement. The position of the tip coincides with one edge of the new aperture.

Our SNOM setup uses  $\lambda = 568$  nm light from a polarized krypton laser (Spectra-Physics Stabilite 2018) passing through a Pockels cell and coupled into the glass fiber illuminating the sample through the TOA probe. Transmitted light is collected by a 0.95 NA objective and passed through a confocal pinhole and a long pass filter to a photomultiplier. The sample is scanned below the probe at constant distance under shear force control using a 100 kHz tuning fork.<sup>21</sup> To prepare the fluorescent sample, a glass cover slide of 20 mm $\times$ 20 mm is rendered hydrophilic in a plasma cleaner. A drop of 40  $\mu\text{l}$  of a 0.5 mg/ml bovine serum albumine solution is applied, and after 2 min the sample is blown dry

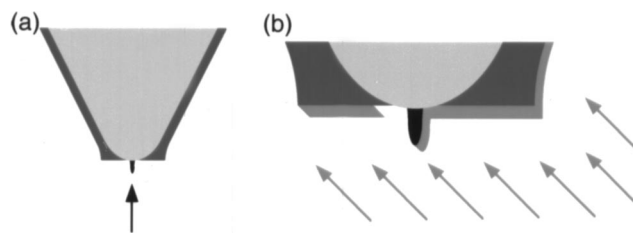


FIG. 1. Schematic steps of fabricating the “tip-on-aperture” (TOA) probe. (a) An EBD tip is grown in a SEM on the aperture of a metallized glass fiber probe; (b) one-sided deposition of Al metallizes the tip and forms an elongated, reduced aperture in the tip shadow.

<sup>a)</sup>Electronic mail: frey@biochem.mpg.de

<sup>b)</sup>Present address: Ludwig-Maximilians-Universität, Sektion Physik, Lehrstuhl Experimentelle Halbleiterphysik, 80539 München, Germany.

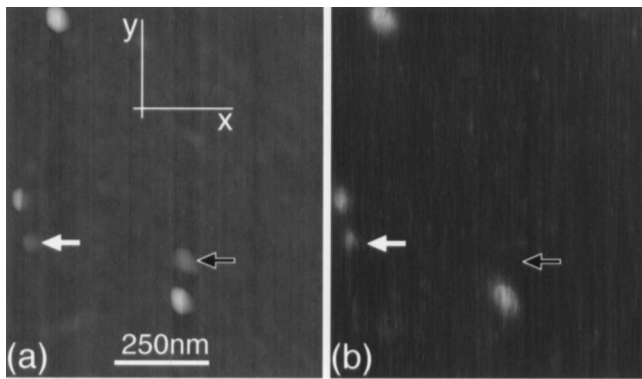


FIG. 2. Images of dye loaded polymer beads (nominal diameter 20 nm), simultaneously taken in (a) topography (height range 32 nm); (b) fluorescence. The scan lines are parallel to the  $y$  axis.

by nitrogen. The resulting layer is used as adhesive to fix red fluorescent (absorption 580 nm, emission 605 nm) carboxylate-modified 20 nm diameter fluorescent beads (microspheres, Molecular Probes). 100  $\mu$ l solution with 0.02% beads is spread over the slide, which is blown dry after 1 min.

Imaging the fluorescent sample with the TOA probe reveals strong optical effects, which are not found without the final metallization of the EBD tip. The bright spots in the fluorescence image [Fig. 2(b)] are similar in size to the elevations in the topographical image found at the same position [Fig. 2(a)], and therefore mark individual fluorescent beads. The line traces (Fig. 3) show that the smallest fluorescent spot (white arrow) measures 25 and 38 nm full width half maximum (FWHM) in two orthogonal directions. The corresponding topographical feature is 5 nm high and measures 40 and 37 nm FWHM, respectively. Differences between the optical and topographical images are expected from the different tip-sample interaction mechanism and from the asymmetric metallization of the EBD tip. The elevation marked by a black arrow has no corresponding spot in the optical image, although it is 8 nm high. This proves that the optical signal above beads is not height induced.

The very high optical resolution is obviously not related to the size of the final aperture, which is 70 nm in length and 30 nm in width, as measured by SEM (Fig. 4). At the distance of 170 nm, given by the measured length of the metal tip, the area illuminated directly from the aperture is quite large. Indeed, around very bright, isolated fluorescing beads, we observe a weakly fluorescing area of about 400 nm width, which vanishes in the background signal for the darker beads in the image shown. The mechanism leading to high optical resolution can be better understood by analyzing measured approach characteristics (Fig. 5). The fluorescence intensity falls rapidly when retracting the tip from a bead. At 5 nm distance it reaches half of its maximum value, proving that

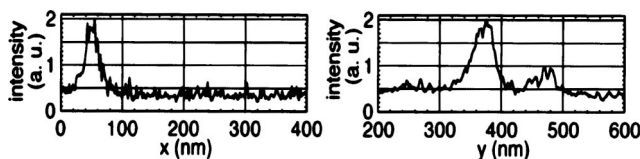


FIG. 3. Orthogonal cross sections through the small fluorescent spot marked by a white arrow in Fig. 2(b) (three lines averaged).

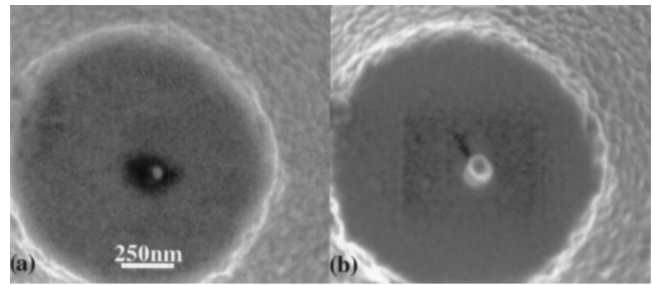


FIG. 4. SEM images of the TOA probe used; (a) before metallization, the EBD tip is seen as bright spot on the dark aperture; (b) after tip metallization and mapping the images of Fig. 2, the slit-shaped aperture is clearly visible. Contamination from previous SEM imaging has enlarged the diameter of the tip and produced the darkened rectangular area.

the optical interaction is highly localized. As the dyes in the beads can be assumed to be randomly oriented, the fluorescence intensity will be proportional to the exciting intensity. The fields of an apertureless probe can be approximated by that of a dipole located in the curvature center of the tip apex.<sup>4,9,11</sup> Outside the tip, its electrical field intensity drops off proportional to  $[(a+z)^{-6} + k^2(a+z)^{-4}]$  along the tip axis, where  $z$  is the distance to the tip apex,  $k = 2\pi/\lambda$ , and  $a$  is the curvature radius. Background intensity can be introduced by an additional constant. This theoretical intensity distance dependence fits well to the measured one when  $a = 35$  nm [Fig. 5(b)], a value which is compatible with the topographical and optical resolution observed, as well as with transmission electron microscope images.

The experimental results of high resolution and steep approach characteristic give evidence that the metallized EBD tip functions as an optical near-field sensor in the same manner as known from apertureless SNOMs.<sup>4-12</sup> Therefore, we expect that other common features will be present with TOA probes, namely, (i) a dominantly  $z$ -oriented polarization of the probing near field<sup>22,23</sup> and (ii) a near-field scattering interaction leading to material contrasts that is well described by an analytic formulation.<sup>5,8,9,23</sup>

What makes the TOA probe superior to other apertureless SNOM probes is primarily its illumination from a spatially fixed, contiguous source. The resulting advantages are compactness of design, stability of the illumination, and reduced background. The short distance from aperture to the tip might be essential for operation in an absorbing liquid.

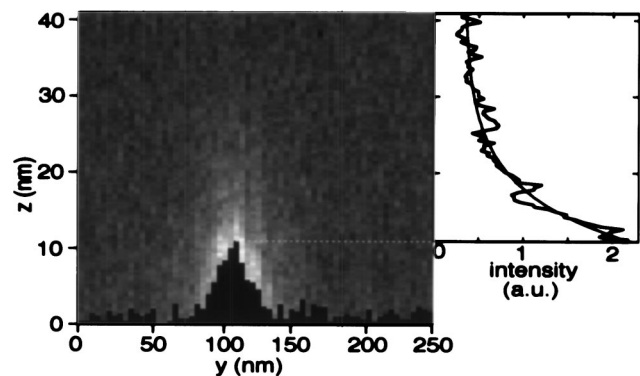


FIG. 5. Fluorescence response ( $y$ - $z$  scan) of the TOA probe above a fluorescent bead. The black structure marks the topography above the bead apex and compares it with dipole theory.

The same advantages also apply, to a collection-mode operation, where the TOA probe couples near-field radiation into the fiber mode, and to a reflection-mode operation.

The configuration presented in this letter has been dictated by practical considerations of fabrication. We are aware that the elongated shape of the aperture with the tip positioned at one edge demands a suitably polarized mode in the glass fiber. Indeed strong influences of polarization were observed both in the near-field and background fluorescence signals, yet their quantification has to await a suitable polarization monitoring scheme which is difficult to perform in our setup with bent fibers. The near-field performance of our TOA probe can be further optimized by tuning the lengths of the metal tip and of the slit aperture, the latter by positioning the tip outside the center of the original aperture and by changing the incidence angle of metal deposition (Fig. 1). Also, different geometries of aperture and tip position can be considered. Fabricating similar TOA tips on other types of aperture probes seems straightforward, for example, on cantilevered aperture tips.<sup>24</sup> In contrast, schemes where single metal grains are picked up on aperture tips<sup>25,26</sup> seem less well suited for a controlled optimization of the near-field strength and confinement. Complete coating of glass tips seems a promising, not yet systematically explored alternative.<sup>17,27</sup>

In conclusion, the tip-on-aperture optical probe has been shown to achieve ultraresolution SNOM imaging, demonstrating a 25 nm FWHM image of a small fluorescing bead at a low level of fluorescence background. Improved performance can be expected from sharper tips and an optimized tip/aperture configuration.

The authors thank R. Hillenbrand, T. Taubner (both Martinsried), and R. Saykally (Berkeley) for stimulating discussions. This work was supported by the Deutsche Forschungsgemeinschaft (SFB 486 and 563).

- <sup>1</sup>H. Bethe, Phys. Rev. **66**, 163 (1944).
- <sup>2</sup>B. Hecht, B. Sick, U. P. Wild, V. Deckert, R. Zenobi, O. J. F. Martin, and D. W. Pohl, J. Chem. Phys. **112**, 7761 (2000).
- <sup>3</sup>S. Kawata and Y. Inouye, Ultramicroscopy **57**, 313 (1995).
- <sup>4</sup>F. Zenhausern, Y. Martin, and H. K. Wickramasinghe, Science **269**, 1083 (1995).
- <sup>5</sup>R. Hillenbrand and F. Keilmann, Appl. Phys. Lett. **80**, 25 (2002).
- <sup>6</sup>G. Wurtz, R. Bachelot, and P. Royer, Eur. Phys. J.: Appl. Phys. **5**, 269 (1999).
- <sup>7</sup>R. Hillenbrand and F. Keilmann, Phys. Rev. Lett. **85**, 3029 (2000).
- <sup>8</sup>M. Labardi, S. Patane, and M. Allegrini, Appl. Phys. Lett. **77**, 621 (2000).
- <sup>9</sup>R. Hillenbrand, B. Knoll, and F. Keilmann, J. Microsc. **202**, 77 (2001).
- <sup>10</sup>E. J. Sánchez, L. Novotny, and X. S. Xie, Phys. Rev. Lett. **82**, 4014 (1999).
- <sup>11</sup>H. F. Hamann, A. Gallagher, and D. J. Nesbitt, Appl. Phys. Lett. **76**, 1953 (2000).
- <sup>12</sup>T. J. Yang, G. A. Lessard, and S. R. Quake, Appl. Phys. Lett. **76**, 378 (2000).
- <sup>13</sup>A. Kramer, W. Trabesinger, B. Hecht, and U. P. Wild, Appl. Phys. Lett. **80**, 1652 (2002).
- <sup>14</sup>F. Keilmann and R. Guckenberger, German Patent No. DE 195,22,546 (1995).
- <sup>15</sup>T. Matsumoto, T. Ichimura, T. Yatsui, M. Kourogi, T. Saiki, and M. Ohtsu, Opt. Rev. **5**, 369 (1998).
- <sup>16</sup>F. Keilmann, J. Microsc. **194**, 567 (1999).
- <sup>17</sup>L. Novotny, D. W. Pohl, and B. Hecht, Ultramicroscopy **61**, 1 (1995).
- <sup>18</sup>D. W. Pohl, *Near-Field Optics, Principles and Applications, Proceedings of the Second Asia-Pacific Workshop* (World Scientific, Singapore, 2000).
- <sup>19</sup>S. Monobe and M. Ohtsu, J. Lightwave Technol. **14**, 2231 (1996).
- <sup>20</sup>K. I. Schiffmann, Nanotechnology **4**, 163 (1993).
- <sup>21</sup>K. Karrai and R. D. Grober, Appl. Phys. Lett. **66**, 1842 (1995).
- <sup>22</sup>L. Aigouy, A. Lahrech, S. Grésillon, H. Cory, A. C. Boccara, and J. C. Rivoal, Opt. Lett. **24**, 187 (1999).
- <sup>23</sup>B. Knoll and F. Keilmann, Nature (London) **399**, 134 (1999).
- <sup>24</sup>E. Oesterschulze, O. Rudow, C. Mihalcea, W. Scholz, and S. Werner, Ultramicroscopy **71**, 85 (1998).
- <sup>25</sup>J. Koglin, U. C. Fischer, and H. Fuchs, Phys. Rev. B **55**, 7977 (1997).
- <sup>26</sup>O. Sqalli, M.-P. Bernal, P. Hoffmann, and F. Marquis-Weible, Appl. Phys. Lett. **76**, 2134 (2000).
- <sup>27</sup>M. Freyland, H. Gersen, H. Heinzelmann, G. Schürmann, W. Noell, U. Staufer, and N. F. de Rooj, Appl. Phys. Lett. **77**, 3695 (2000).